Hindawi
Advances in Civil Engineering
Volume 2023, Article ID 6357539, 11 pages
https://doi.org/10.1155/2023/6357539

Research Article

Closure Scheme Analysis of 3 × 70 m Bearingless Integral Rigid Frame Bridge of Fuzhou Xiamen High-Speed Railway

Fangwen Weng[1] **and Xiangui Li**[2]

[1]*CCCC Second Harbor Engineering Company Ltd., Wuhan 430040, China*
[2]*Southeast Coastal Railway Fujian Company Ltd., Fuzhou 350013, China*

Correspondence should be addressed to Fangwen Weng; sponerock@hbut.edu.cn

Received 6 September 2022; Revised 28 October 2022; Accepted 24 November 2022; Published 30 March 2023

Academic Editor: S. Mahdi S. Kolbadi

The hydrodynamic problems associated with the construction of the sea-crossing bridge were proposed. The deep-water approach bridge on both sides of the main bridge of Fuzhou Xiamen high-speed railway adopts the bearingless prestressed concrete integral rigid frame bridge for the first time in the domestic railway bridge design. The rigid frame bridge applies the hanging basket cantilever construction, and there are several options for closure. Because the bridge structure system changes before and after closure, which will cause the redistribution of bridge internal force, the results of internal force redistribution will be different with the sequence and position of closure, and sometimes, there will be great changes. In order to select the optimal closure scheme, this article establishes the finite element model of the whole bridge and analyzes the whole construction process according to the working conditions and the mechanical state of the bridge before closure is obtained. Based on this state, eight closure schemes are analyzed and studied, which provides a sufficient mechanical basis for the determination of the final closure construction scheme.

1. Project Profile

1.1. Rigid Frame Bridge Introduction. On both sides of the main bridge of Quanzhou Bay Sea-crossing Bridge, there are some built continuous rigid frame bridges with one link of three spans and each span of 70 m. There are 9 continuous rigid frame bridges from pier 47 to 74 on the Fuzhou side, 11 continuous rigid frame bridges from pier 79 to pier 114 on the Xiamen side, and also another continuous rigid frame bridge of 2 × 70 m on the Xiamen side. The double-limb thin-walled pier is designed in the piers connecting the two ends of the continuous rigid frame bridge with other bridges and the two adjacent connecting piers of the continuous rigid frame bridge. The hollow pier is used in the middle of each pier, and the pier height is 27 m–51 m. The continuous rigid frame bridge adopts the cross-section form of a concrete variable cross-section box girder, which is a prestressed concrete integral rigid frame bridge without support. It is first used in domestic railway bridges, and the whole bridge does not have the bridge bearing.

According to the stress and construction characteristics of multispan multiconnected continuous rigid frame bridge, there are many times of structural system conversion, difficult construction alignment control, and the complex process in the construction process. Reasonable selection of the closure sequence of multispan multiconnected continuous beam construction is an important guarantee for structural quality and shape control. The advantages of such structural solution include better seismic performance and convenience in construction [1].

1.2. Technical Status of the Integral Rigid Frame Bridge without Bridge Bearing. Actually, the environment impact was simulated before the bridge construction in 1993 [2]. However, negligible change was predicted by the crude numerical model, which was newly developed at that stage. At present, the development of continuous rigid frame bridges in China and abroad tends to increase the span and joint length, and the research focuses are basically on the

construction optimization and monitoring of long-span and long-joint rigid frame bridges [3]. At present, there are no such cases of multiconnected continuous rigid frame without support in China and abroad, and the research on its complete set of construction technology is blank, most of which are simply repeated by single connection [4].

Semi-integral bridges have been widely used in German high-speed railways, such as the Erfot–Haller/Leipzid Railway Line and the Wendlingen–Ulmd Railway Line. The pier of semi-integral railway bridge is integrally connected with the superstructure, but the superstructure still sets the bridge bearing at the abutment. At present, the construction of this kind of bridge has been realized for the semi-integral railway bridges without structural expansion joints and rail expansion regulator within the length of 580 m [5].

The integral rigid frame bridge has no bridge and the side pier and the middle pier are consolidated with the main beam to form a rigid frame structure. The super- and substructures can cooperate, and the resistance of each part is evenly and fully, which realizes the overall stress of the structural system. The amount of material is greatly reduced, the structure is light and beautiful, good seismic performance, less maintenance, economy, and durability. Among the existing railway bridges in China, there is no precedent for the application of integral rigid frame bridge without bridge bearing.

2. Continuous Rigid Superstructure Closure Scheme

2.1. Overview of Mechanical Properties of Multiconnected Continuous Rigid Frame Bridge. The structure form of 3×70 m continuous rigid frame bridge is relatively novel, and the joint and joint connection position does not set bridge bearing. The junction pier is a double-legged pier, and the main beam at the top of the pier is divided, where expansion joints are set. During construction, both sides of the handover pier are temporarily consolidated, which facilitates the use of double-cantilever construction. It is conducive to reducing the construction difficulty and the use of temporary structures. After the completion of the construction, the structural system is transformed to remove the temporary consolidation [6].

The design and construction scheme of the transition pier is very characteristic, the main beam and pier are still consolidated, but the center of the pier is divided into two parts along the transverse. The construction made full use of the characteristics of the structure. Through the temporary anchoring structure to form an independent force structure, the construction method can be optimized. However, this design and construction scheme will also put forward higher requirements for the temporary anchorage technology, cantilever casting construction technology, construction control technology, construction process organization, closure sequence determination, and other aspects. In this article, the influence of different closure sequence on the mechanical properties of bridges is compared and analyzed.

The closure process of a continuous rigid frame bridge is not only the process of structural system transformation but also the process of bridge completion in the final stage of cantilever construction. After closure, the bridge structure will change from the previous static structure to the statically indeterminate structure, and the internal force will be redistributed. Different closure sequences will lead to great differences in the redistribution of internal force, thus affecting the mechanical properties of the entire bridge.

2.2. Closure Construction Scheme. In this article, taking the Fuzhou side from no. 47 pier to no. 74 pier, a total of 9 links and 27 spans as the research objects for the comparison of the closure scheme, 8 closure schemes are analyzed and compared in order to fully understand the advantages and disadvantages of closure schemes.

In order to shorten the construction period, the middle pier of each joint and the adjacent joint transfer pier are simultaneously cantilevered. When the maximum cantilever state is reached, there are three closure joints in each joint. For the ease of distinction, each joint pier number is numbered in the order of 1, 2, and 3 from the Xiutu port to Quanzhou Bay (for example, joint port number A1 is A1-1, A1-2, A1-3), as shown in Figure 1.

With the center on the A5 joint, the closures were carried out simultaneously in the two directions of Xiutu Port Coast and Quanzhou Bay. The construction of transportation infrastructure is a vital step in boosting economic and social opportunities and often results in land use changes. According to the four principles of "first side span and then middle span," "first middle span and then side span," "alternate closure of side and middle span," and "closure in turn," the nine joint were divided into three construction bid sections (A1, A2, and A3 were bid Section 1; A4, A5, and A6 were bid Section 2; and A7, A8, and A9 were bid Section 3), and eight closure schemes were formulated. In each closure scheme, the prestressed tendons of the temporary cantilever beam are removed after the closure of the closure openings on both sides of the transfer pier. The side span closure beams are tensioned in two batches. The first batch is tensioned after the closure of the side span, and the second batch is tensioned after the removal of the temporary prestressed tendons. Three construction bid sections are shown in Figure 2.

When multiple beams are continuously connected, the piers are used as the intermediate supports. However, the distance between piers needs to be carefully calculated because it would affect the solidity of the bridge. The construction of a beam bridge essentially adds a significant structure in a form of a large steel or iron beam called a girder. The girder provides a stronger support to the concrete deck and transfers the load down to the foundation. Generally, there are two types of broadly used girders including I-beam girders and box girders [7]. The scheme one to scheme four in the eight kinds of the closure scheme take three sections as a whole construction, including 22 steps; scheme five to scheme eight will construct three sections simultaneously, including nine steps shown as follows.

The closure mode of scheme one is side and middle span alternate closure; the closure mode of scheme two is in turn

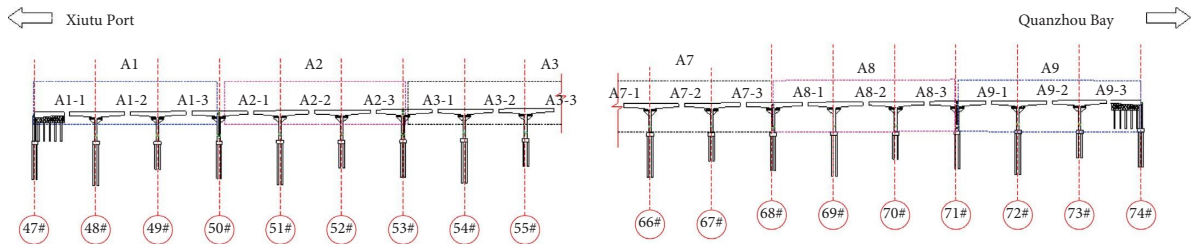

Figure 1: Number of each joint closure entrance.

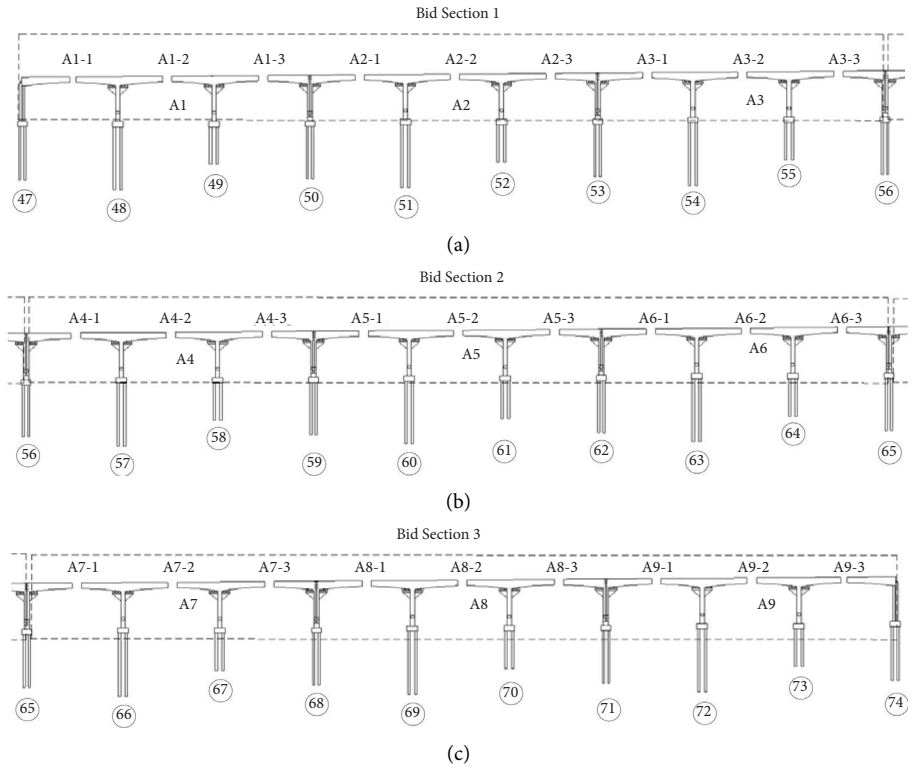

Figure 2: Three construction bid sections are (a) bid section 1, (b) bid section 2, and (c) bid section 3.

closure; the closure mode of scheme three is first middle span and then side span; the closure mode of scheme four is first side span and then middle span; the closure mode of scheme five is the simultaneous side and middle span alternate closure with three construction bid sections as a unit; the closure mode of scheme six is that three construction bid sections are taken as a unit to close at the same time; the closure mode of scheme seven is that the three construction bid sections are taken as a unit at the same time, first middle span and then side span; and the closure mode of scheme eight is that three construction bid sections are taken as a unit at the same time, and the side span is first and then the middle span.

It is proposed that the construction time of each closure section is 7 days, the removal time of temporary prestressed tendons is 2 days, and the tension time of the second batch of side span closure prestressed tendons is 2 days. Table 1 shows the maximum span number and closure time in the closure process of the 8 schemes.

3. Numerical Simulation Analysis of the Continuous Rigid Frame in the Construction Stage

A continuous rigid frame bridge cantilever construction process is very complicated and needs a high degree of internal force and deformation control. The internal force and deformation as the construction of the advance will be affected by many factors, and those factors include material elastic modulus, bulk density, temperature, shrinkage and creep, and external load [8]. These effects directly lead to the change of the internal force and deformation. Besides, there are also many structural system changes in the construction and structural system. Therefore, it is very necessary to conduct an accurate theoretical calculation and analysis before the construction.

The results of calculation and analysis can greatly guide the construction control, and the calculation model can also continue to play an important role in the construction

Table 1: The closure scheme duration and the maximum span number in the closure process.

Construction schemes	Closure construction period (days)	Maximum span number in the closure process	Timing of maximum spans
Scheme 1	114	7	A4-3 and A6-1 closure
Scheme 2	114	5	A4-3 and A6-1 closure
Scheme 3	114	7	A4-3 and A6-1 closure
Scheme 4	114	3	A5-2 closure
Scheme 5	43	7	A1-3, A3-1, A4-3, A6-1, A7-3, and A9-1 closure
Scheme 6	43	5	A1-3, A3-1, A4-3, A6-1, A7-3, and A9-1 closure
Scheme 7	43	7	A1-3, A3-1, A4-3, A6-1, A7-3, and A9-1 closure
Scheme 8	43	3	A2-2, A5-2, and A8-2 closure

monitoring, which can obtain dynamic feedback and decision-making in order to achieve the design purpose [9]. The final closure of the long-span continuous rigid frame is a structural system change, the final closure of the whole structure can produce dramatic change of internal force and deformation, and the final closure of the structure state (internal force and deformation) are the results of each construction stage accumulation. Therefore, for studying the mechanical state of the bridge structure during closure, it is necessary to analyze all the previous construction stages clearly. Before closure, each joint will undergo eight construction stages to form the maximum cantilever state before closure as shown in Figure 2, and the single joint as shown in Figure 3:

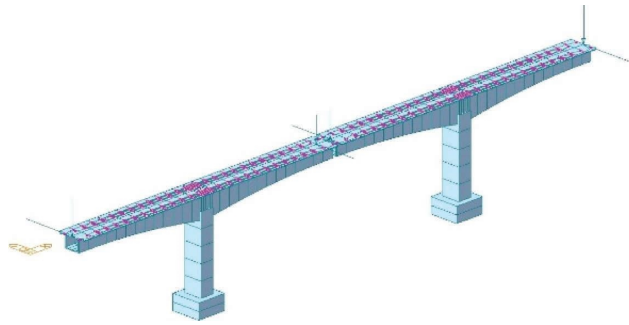

Figure 3: Phase VIII construction.

3.1. Establishment of the Finite Element Model. Piers for integral bridges can be of any type. If the inherent flexibility of a chosen type will accommodate structural movements, the piers may be built integrally with the superstructure or connected to it with anchor bolts. Otherwise, piers are designed as semirigid self-supporting substructures with movable bearings between them and the superstructure [10]. The finite element model adopts the beam element. In the bridge span direction, the variable section group provided by the program is used to generate variable section beams, and the beams and piers are consolidated. The beam pier corresponding node uses the master-slave node for rigid connection. The joints at the bottom of the pier are fixed boundary conditions with six degrees of freedom [11]. The loads in the construction process include dead weight, construction load, hanging basket weight, which is 75 tons, and the second-phase dead load. The influence of concrete shrinkage and creep is considered in calculation. The shrinkage and creep are calculated according to the code. The temperature load is taken according to the specification, and the temperature of the system is considered as +15°C or −15°C. The material parameters are shown in Table 2; the material parameters of a prestressed steel beam are shown in Table 3.

Table 2: Material characteristics of prestressed concrete.

Material properties	Values
Elastic modulus	36000 MPa
Weight by volume	26.5 KN/m
Thermal expansion ratio	0.00001
Poisson ratio	0.18
Prestressed concrete strength	≥95%

The number of prestressed steel beams is large, the shape is complex, and the conventional modeling method is time-consuming and laborious [12]. In the calculation, the interface program is developed to connect finite element software with three-dimensional modeling software. The spatial curve model of prestressed steel bundle can be established in 3D software and then directly imported into the finite element software through the interface program, which greatly improves the modeling efficiency of prestressed steel bundle. The whole finite element model is shown in Figure 4.

3.2. Results Analysis. The cantilever construction is carried out at the same time for the middle pier and the junction pier. The vertical deformation diagram and bending moment diagram of the structure under the maximum cantilever state are shown in Figures 5 and 6. The maximum span involved in the construction process of different closure schemes is 7 spans, and the influence of different closure schemes on other joint internal forces is similar to A4 and A5.

3.2.1. Contrastive Analysis of Internal Force of Each Closure Scheme. In the process of the construction and in the complete stage of the bridge, the beam sections in the position of the pier and closure are prone to bending cracks. The main beams at the junction pier, middle pier, and closure section are taken as stress statistical points to

Table 3: Properties of prestressed tendons.

Mechanical properties of prestressed reinforcement	Numerical magnitude
Elastic modulus (Ep)	195000 MPa
Duct deviation coefficient	0.0015
Relaxation coefficient of steel strands	0.3
Friction coefficient of prestressed duct	0.17
End-anchorage reinforcement recondensation	0.006 m
Controlled stretching stress of longitudinal steel strands	1395 MPa
Controlled stretching stress of lateral steel strands	1302 MPa
Controlled stretching stress of vertical steel strands	785 MPa

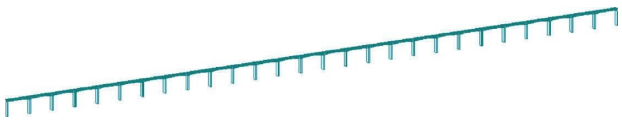

Figure 4: Nine-link 3×70 m continuous rigid frame 3D finite element model.

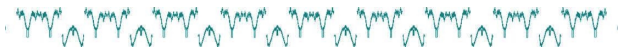

Figure 5: Vertical deformation diagram of the maximum cantilever state.

Figure 6: Bending moment diagram under the maximum cantilever state.

compare and analyze the stress in the construction process and in the complete stage of the bridge of different closure schemes, as shown in the figure.

Midas-Civil finite element software can output the normal stress at four positions of the upper and lower flange of the beam element section [13]. The maximum compressive stress and tensile stress (the compressive stress is negative and the tensile stress is positive) at four positions of the upper and lower flange are only counted when the beam element stress of different closure schemes is calculated, as shown in Figures 7 and 8.

The stress difference $\Delta\sigma$ is used to describe the bridge completion state and the stress deviation in the closure process between the schemes, as shown in the following formula:

$$\Delta\sigma = \sigma_{\max} - \sigma_{\min}. \quad (1)$$

In the formula, $\sigma_{\max}$ represents the maximum stress of the beam element at a certain position in eight construction schemes and $\sigma_{\min}$ represents the minimum stress of the beam element at a certain position in eight construction schemes.

The comparison results of the bridge completion state and maximum stress in the closure process of eight closure schemes are shown in Figures 9 and 10 and Tables 4 and 5.

Based on the above data analysis, it can be seen that

(1) In the completed bridge state, there is little difference in the stress between different closure schemes, and both the pier and closure section present the full section compression state. The maximum stress difference $\Delta\sigma$ of the eight schemes is 0.42 MPa, which appears at the beam pier section of the midspan pier of the bridge link A4 (SA4-2-3).

(2) During the closure process, the tensile stress occurs at the beam section of the middle pier and the junction pier, and the beam section of the closure section is in a compression state. Among them, the tensile stress of the beam section (SA4-2-3) at the middle span pier of scheme 1 and scheme 5 in the link A4 is the largest, 1.53 MPa and 1.68 MPa, respectively.

(3) In the construction of different closure schemes, the maximum stress difference $\Delta\sigma$ is 1.04 MPa, which appears at the closure section pier of the link A4 span (SA4-1-2). In the process of closure, the maximum stress difference $\Delta\sigma$ is 0.78 MPa, which appears at the beam section midspan pier of the link A4 (SA4-2-3).

3.2.2. Comparative Analysis on Structural Deformation of the Bridge Completion State of Each Closure Scheme. In the construction process, the precamber is generally used to make the structure achieve reasonable completed bridge shape. In the case that the longitudinal slope and long-term deflection effect of the structure are not considered, it can be considered that the reasonable completed bridge shape of the structure is when the deflection of each point in the completed bridge state is 0. As the girder deflection at the pier is generally zero and the deflection at the closure is large, the deflection of the bridge at the A4 joint and A5 joint is taken as a comparative analysis of the parameters deviating from the reasonable completed bridge state under different closure schemes, as shown in Figure 11.

The average deflection D_{avg} at each deflection statistical point under the bridge completion state represents the deviation of bridge completion deflection from the reasonable bridge completion state of different schemes, which actually reflects the average camber of each statistical point in the construction process, as shown in the following formula:

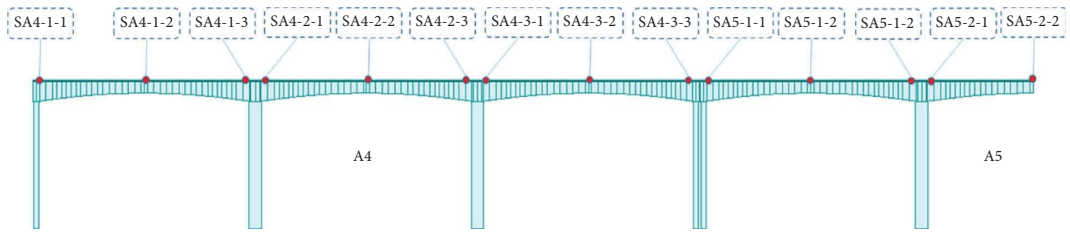

Figure 7: Beam element stress statistical point.

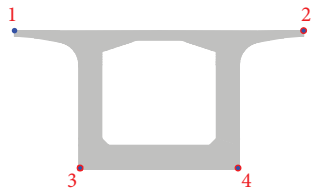

Figure 8: Finite element stress calculation output point.

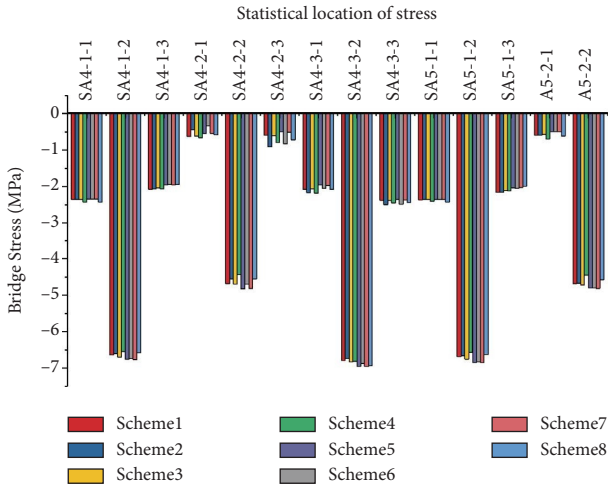

Figure 9: Comparison of beam element stress of each closure scheme in the bridge forming stage.

$$D_{\text{avg}} = \frac{|D_1 - 0| + |D_2 - 0| + \ldots |D_9 - 0|}{9}. \quad (2)$$

In the formula, D_i is the deflection of 9 statistical points of deflection.

Based on the above data analysis as shown in Table 6 and Figure 12, it can be seen that

(1) Scheme 4 and scheme 8, scheme 2 and scheme 6, scheme 1, scheme 3, scheme 5, and scheme 8 are relatively close in the bridge alignment

(2) There is little difference between the maximum deflection and the maximum arch under different closure schemes. The maximum deflection of each closure scheme in the completed bridge state is about 20 mm, which all appear at the right position of the closure section of A4 joint third span (DA4-3-2). Except for scheme 4 and scheme 8, the maximum camber appears on the left side of the third span closure section, and the maximum cambers of other closure schemes in the bridge state all appear on the left side of the A4 middle span closure section (A4-2-1). The maximum camber of scheme 4 and scheme 8 is about 5 mm, and the maximum camber of other schemes is about 10 mm.

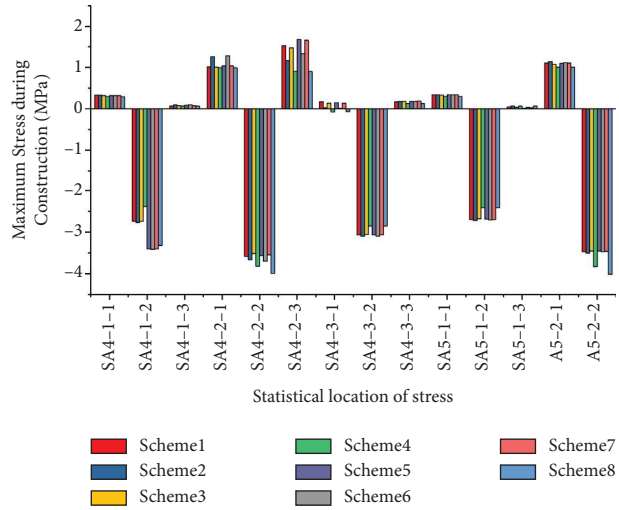

Figure 10: Comparative analysis of maximum stress of the beam element in the closure process of different closure schemes.

(3) The D_{avg} value of average deflection of all closure schemes in the completed bridge state is not different from each other. Compared with other closure schemes, the scheme 4 and the scheme 8 are close to reasonable completed bridge shape. Scheme 4 has the lowest D_{avg} value of average deflection of 6 mm, while scheme 5 and scheme 7 have the largest D_{avg} value of 10.5 mm. The D_{avg} value difference between the maximum and minimum average deflections is 4.5 mm.

(4) In conclusion, the difference of internal force and bridge shape between different closure schemes is small. There is little difference between the maximum stress of the main beam in the process of closure and the stress in the completed bridge state between different closure schemes. The maximum upper deformation, deflection, and D_{avg} value of average deflection between different closure schemes are within 5 mm.

Table 4: The bridge state and the stress difference between the schemes in the process of closure (MPa).

Construction scheme	Statistical number of beam element stress													
	SA4-1-1	SA4-1-2	SA4-1-3	SA4-2-1	SA4-2-2	SA4-2-3	SA4-3-1	SA4-3-2	SA4-3-3	SA5-1-1	SA5-1-2	SA5-1-3	A5-2-1	A5-2-2
$\Delta\sigma$	0.08	0.23	0.13	0.33	0.39	0.42	0.22	0.23	0.13	0.07	0.29	0.17	0.20	0.36

Table 5: Maximum stress difference of the beam element in the closure process of different closure schemes (MPa).

Construction scheme	Statistical number of beam element stress													
	SA4-1-1	SA4-1-2	SA4-1-3	SA4-2-1	SA4-2-2	SA4-2-3	SA4-3-1	SA4-3-2	SA4-3-3	SA5-1-1	SA5-1-2	SA5-1-3	A5-2-1	A5-2-2
$\Delta\sigma$	0.04	1.04	0.04	0.29	0.48	0.78	0.25	0.25	0.06	0.05	0.31	0.05	0.13	0.57

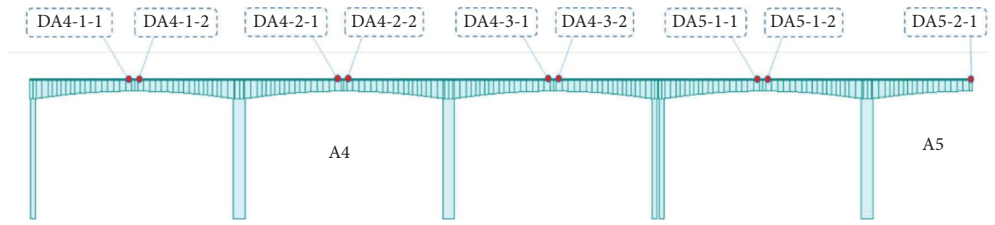

Figure 11: Deformation statistical point.

Table 6: Average deflection of each closure scheme in the bridge state (mm).

Closure schemes	D_{avg}
Scheme 1	9.8
Scheme 2	9.3
Scheme 3	9.8
Scheme 4	6
Scheme 5	10.5
Scheme 6	9.8
Scheme 7	10.5
Scheme 8	6.3

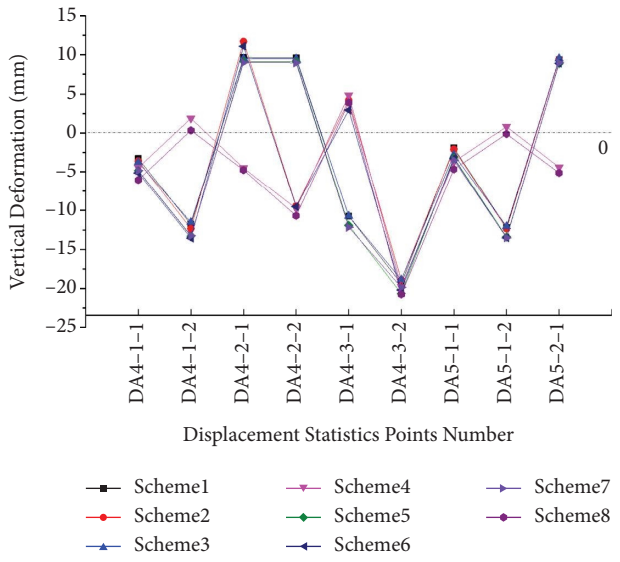

Figure 12: Deviation of the displacement statistical point.

3.2.3. Stress Analysis of Each Closure Scheme under Ambient Temperature Change. Studies attempting to relate environmental factors to bridge temperatures, and subsequently to bridge movements and stresses, indicate that the task is extremely complex [14]. Due to the temporary connection between the box girders on both sides of the junction pier, the force of the structure is different from that of the conventional continuous rigid frame. The more spans are in the closure process, the more obvious the effect of the structure is under the temperature change. The difference between temperature rise and temperature drop in the closure process is proposed to be 15°C. In the closure process of scheme 1, the maximum number of spans is 7 and the structural stress diagram under the effect of temperature rise and temperature drop is shown in the figure. Table 7 and Figure 13 show the statistical results of maximum stress of main beams and piers of the link A4 and A5 during the construction stage of the maximum span number involved in the closure process of different closure schemes.

According to the Table 7, it can be seen that

(1) Compared with the temperature rise of ambient temperature, the temperature drop of ambient temperature has a greater impact on the stress of structural piers and girders

(2) The influence of ambient temperature on the stress of the girder and pier during construction is related to the maximum span number in the process of closure, but there is no direct proportional relationship between the maximum span number in the process of closure of different closure schemes and the maximum stress of girder and pier considering the effect of temperature. Among them, the effect of environmental temperature on scheme 1, scheme 3, scheme 5, and scheme 7 has a greater impact on the maximum stress of the bridge pier and girder than other closure schemes, and the risk of cracking of the bridge pier and girder is greater. The maximum span number of scheme 1, 3, 5, and 7 is 7, and the maximum stress of the bridge pier and main beam is about 6.5 MPa and 3.6 MPa, respectively. In scheme 2 and 6, the maximum span is 5 spans in the process of closure, and the maximum stress of the bridge pier and main beam is about 3.0 MPa and 2.4 MPa, respectively. The maximum span in scheme 4 and 8 is 3 spans, and the maximum stress of the bridge pier and main beam is about 4.5 MPa and 1.4 MPa, respectively.

(3) The reason why the maximum stress of the pier in scheme 2 and scheme 6 is smaller than that in scheme 4 and 8 is that the side pier section is smaller than the middle pier section in scheme 4 and scheme 8 due to the temporary removal of prestress, and the maximum stress appears on the side pier. After the removal of all temporary prestress in scheme 2 and scheme 6, the maximum span number is 3. The maximum stress of the bridge pier in the process of closure is the same as that in scheme 4 and 6.

(4) This article focuses on the comparison and selection of different closure schemes. In the analysis of the temperature effect, the ambient temperature is 15°C, and the bridge pier height is uniformly set at 40 m. In

Table 7: Each closure scheme considers/does not consider the maximum stress (MPa) of the main beam and pier under the action of temperature.

Closure schemes	Maximum span number in the closure process	Considering the effect of temperature		Not considering the effect of temperature	
		Bridge pier	Main beam	Bridge pier	Main beam
Scheme 1	7	6.1 (1.0)	3.6 (1.3)	2.8	1.3
Scheme 2	5	3.1 (0.9)	2.3 (0.6)	1.2	1.3
Scheme 3	7	6.1 (1.0)	3.6 (1.3)	2.7	1.3
Scheme 4	3	4.3 (2.6)	1.4 (1.3)	2.6	1.3
Scheme 5	7	6.5 (1.0)	3.9 (1.3)	2.8	1.3
Scheme 6	5	3 (0.9)	2.5 (0.6)	1.2	1.3
Scheme 7	7	6.6 (1.0)	3.9 (1.3)	2.7	1.3
Scheme 8	3	4.6 (2.7)	1.4 (1.3)	2.7	1.3

Note. The values in brackets refer to the structural stress at the corresponding position without considering temperature load.

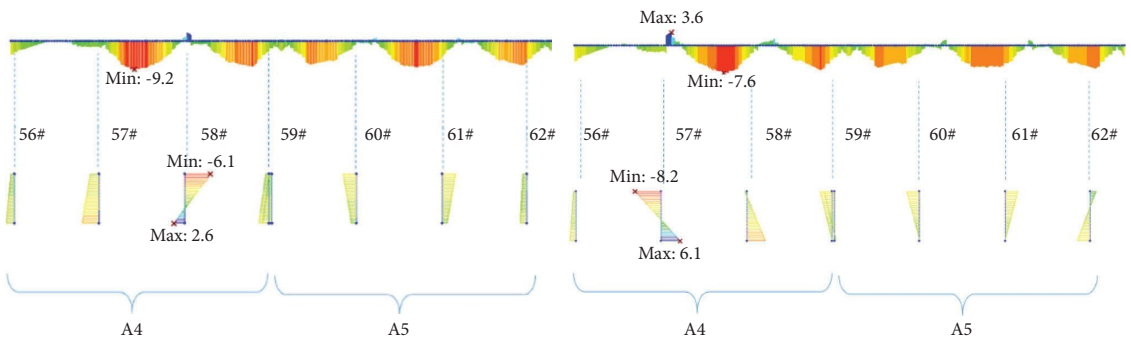

Figure 13: Stress diagram of the girder and pier under temperature rise and drop (MPa).

the checking calculation of structural cracking under the effect of temperature, the actual height of the bridge pier should be considered, and the temperature change at the bridge site should be further investigated.

4. Conclusion

The Quanzhou Bay Bridge of Xiamen High-speed Railway is a steel-concrete composite beam semifloating cable-stayed bridge whose approach bridges contains 9-link 3×70 m rigid frame bridges without bridge bearing. Because there are lots of spans, what the final closure scheme is set might lead to a big impact on the completed bridge. If the appropriate construction scheme is applied, it will be better for releasing the deformation of the beam body, reducing the additional internal force, improving the stress of the girder, and making use of the bridge. On the contrary, if a better construction scheme is not selected at this stage, more additional internal forces and deformation will be accumulated in the beam body, and they will superimpose on the beams together with the operation load resulting in the failure and cracking of the beam body and affecting the operation of the bridge. The results show that the displacement deformation decreases gradually with increasing elastic modulus of the soil around the anchor pier and increases with increasing Poisson's ratio. The change in elastic modulus mainly affects the relative shear displacement of the anchor pier and soil and the compressive deformation of the soil at the front end of the anchor pier. Poisson's ratio has the greatest influence on the relative shear displacement of the anchor pier and soil. A larger anchor pier is not better; thus, it is wise to choose the economic design dimension. Theoretical and numerical simulation results are consistent, showing a linear growth trend.

In this article, 8 kinds of closure schemes are calculated and analyzed, and the following conclusions are drawn:

(1) The differences of structural stress and bridge alignment in the process of closure are small. In the process of closure, the maximum difference of compressive stress, tensile stress, and bridge stress is 1.04 MPa, 0.78 MPa, and 0.42 MPa, and the difference of the D_{avg} value of the average deflection and statistical position of the bridge are within 5 mm.

(2) The influence of ambient temperature on the maximum stress of the pier and girder during construction is more obvious. After considering the effect of temperature, schemes 1, 3, 5, and 7 have a greater risk of cracks in bridge piers and main beams, while scheme 4 and scheme 8 have a smaller maximum stress in the main beam in the process of closure than other schemes, so the risk of cracks is relatively small.

(3) The difference between scheme 4 and scheme 8 mainly lies in the construction organization, and scheme 8 has three construction bid sections. When comparing scheme 4 and scheme 8, something

should be considered comprehensively such as construction period and construction organization.

(4) Through the study of this article, the selection of the bridge closure construction scheme provides a sufficient basis.

Data Availability

The data used to support the findings of this study are included within the article.

Conflicts of Interest

The authors declare that they have no conflicts of interest.

Acknowledgments

This study was supported by the Project of Science and Technology Research and Development Plan of China Railway Corporation (K2018G017).

References

[1] E. F. Deng, L. Zong, Y. Ding et al., "Seismic performance of mid-to-high rise modular steel construction-A critical review," *Thin-Walled Structures*, vol. 155, Article ID 106924, 2020.

[2] B. Peeters and G. De Roeck, "One-year monitoring of the Z24-Bridge: environmental effects versus damage events," *Earthquake Engineering & Structural Dynamics*, vol. 30, no. 2, pp. 149–171, 2001.

[3] Y. Sheng and O. Jinping, "Structural health monitoring and model updating of aizhai suspension bridge," *Journal of Aerospace Engineering*, vol. 30, 2016.

[4] S. Deshan, L. Qiao, K. Inamullah, and Z. Xiaohang, "A novel finite element model updating method based on substructure and response surface model," *Engineering Structures*, vol. 103, 2015.

[5] S. X. Rong and S. H. Yu, "The confirmation of closure jacking force in continuous rigid frame bridge," *Applied Mechanics and Materials*, vol. 638, 2014.

[6] R. W. Li, F. S. Zhong, B. J. Xiao, D. G. Wei, and Y. Z. Jia, "Analysis on construction control of continuous rigid frame bridge in winter intermission," *Advanced Materials Research*, vol. 791–793, 2013.

[7] H. D. Wright, H. R. Evans, and P. W. Harding, "The use of profiled steel sheeting in floor construction," *Journal of Constructional Steel Research*, vol. 7, no. 4, pp. 279–295, 1987.

[8] Q. Zhu, Y. L. Xu, and X. Xiao, "Multiscale modeling and model updating of a cable-stayed bridge. I: modeling and influence line analysis," *Journal of Bridge Engineering*, vol. 20, 2014.

[9] S. Masoud, G. R. Imbaro, J. A. McClain, and L. C. Brown, "Structural model updating using experimental static measurements," *Journal of Structural Engineering*, vol. 123, no. 6, 1997.

[10] N. T. Davis, E. Hoomaan, M. Sanayei, A. K. Agrawal, and F. F. Jalinoos, "Integrated superstructure-substructure load rating for bridges with foundation movements," *Journal of Bridge Engineering*, vol. 23, no. 5, Article ID 04018022, 2018.

[11] M. Y. Fattah, K. T. Shlash, and M. S. Al-Soud, "Pile-clayey soil interaction analysis by boundary element method," *Journal of Rock Mechanics and Geotechnical Engineering*, vol. 4, no. 1, 2012.

[12] R. M. Antonio and M. Valdés, "Long-term behavior of continuous precast concrete girder bridge model," *Journal of Bridge Engineering*, vol. 5, no. 1, 2000.

[13] M. R. Chowdhury and J. C. Ray, "Further considerations for nonlinear finite-element analysis," *Journal of Structural Engineering*, vol. 121, no. 9, pp. 1377–1379, 1995.

[14] J. C. Reynolds and J. H. Emanuel, "Thermal stresses and movements in bridges," *Journal of the Structural Division*, vol. 100, no. 1, pp. 63–78, 1974.